Scientific
Research
Publishing

Overview of Tide Characteristics in Cameroon Coastal Areas Using Recent Observations

R. Onguene[1,2,3]*, E. Pemha[4], F. Lyard[2], Y. Du-Penhoat[2], G. Nkoue[5], T. Duhaut[3], E. Njeugna[1], P. Marsaleix[3], R. Mbiake[1], S. Jombe[6], D. Allain[2]

[1]Multidisciplinary Climate Change Research Laboratory, University of Douala, Douala, Cameroon
[2]LEGOS/OMP UMR 5566 (CNES-CNRS-IRD-UPS), Toulouse, France
[3]Laboratoire d'Aérologie, CNRS and Toulouse University, Toulouse, France
[4]Laboratory of Applied Mechanics and Hydraulic, Faculty of science, University of Yaounde I, Yaounde, Cameroon
[5]Faculty of Science, University of Douala, Douala, Cameroon
[6]DOUALA Harbour, Douala, Cameroon
Email: *ziongra@yahoo.fr, portdouala@iccnet2000.com

Abstract

Time series of sea level heights have been collected at different stations along the Cameroon coast. The dataset covers a period ranging from 2007 to 2012. Tide data measured by float type recorders have been digitalized and quality-controlled with tools developed at Laboratoire d'Etudes Géophysique et Océanographie Spatiale (LEGOS). Short gaps in the data have been interpolated while large gaps were not. Tide constituents were retrieved through harmonic analysis using 123 waves having a period ranging from long ones to eighth-diurnal ones. The reconstructed signal is used to assess the quality of both the data and the analysis and the erroneous records were examined and corrected. The effect of the hourly averaging of the raw data on the quality of the analysis is also investigated. The tide constituents having the largest amplitudes are, as expected, the semi-diurnal, diurnal, fourth-diurnal and long term constituents. The major components of semi-diurnal waves are the M2 and S2 tides. The M2 tide height ranges between 0.5 and 0.85 m. The maximum height is found at Cameroon estuary and the minimum at the Kribi station located in the South coast. The S2 constituent varies similarly as the M2 constituent. Its amplitude ranges between 0.18 and 0.52 m. The lowest S2 amplitude occurs also at Kribi station. In the Dibamba estuary the spectrum shows a larger number of significant semi-diurnal and fourth-diurnal waves than other zones. Concerning diurnal waves, the dominant one is the K1 tide and its amplitude is homogeneous along the coast. The influence of the long-term components is the strongest in the Cameroon

---

*Corresponding author.

estuary due to important fluctuations of the rivers run-off.

Keywords

1. Introduction

The Cameroon coast is a zone where important industrial and environmental interests are located. Cameroon, as its neighbouring countries, is an important offshore oil and gas producer. The Cameroon government also invests in important marine projects like the industrial Kribi harbour complex and the marine protected areas of Kribi-Campo and Mouanko. Moreover, the country faces other problems in coastal areas like salinity intrusion and sediment transport increase in Cameroon estuary, which are probably linked to climate change [1]. All these issues led to an increasing interest in the understanding of the local coastal dynamics and especially tides.

Geographically, the coast of Cameroon is connected to the equatorial Atlantic Ocean. The shoreline spreads over 400 km (8.3°E - 10.15°E and 3.3°N - 5°N) (**Figure 1**) between Idenau and Campo. The littoral zone presents an array of varying geomorphological attributes consisting of creeks, lagoons, sand and rocky beaches, coastal plains, wetlands and mangroves [2]. These varying landforms include the Cameroon estuary which has the particularity to be a vast delta where three important rivers join. The tides of the Cameroon coast have been described by many authors but little attention has been given to the tide components. Most of these studies are very descriptive. [3] shows that tides are meso-tidal with the maximum tidal range of 3 m. According to [4] [5] tides in Cameroon estuary are semi-diurnal and very asymmetric.

The signal variations in the Kribi zone suggest that the diurnal constituents are higher in this region. In the Cameroon estuary, and more specifically in the Dibamba and Wouri estuaries, an investigation realized by [6] shows that the tide amplification depends mostly on convergence shapes. However, none of these studies presents a harmonic analysis of tide data. This paper aims to investigate the tidal constituents using the harmonic analysis method in the Cameroon coastal areas in order to perform a tide prediction.

The data in this region is scarce and not homogeneously distributed. The research collaboration between the University of Douala, Douala harbour and LEGOS in France has allowed creating a database including all the
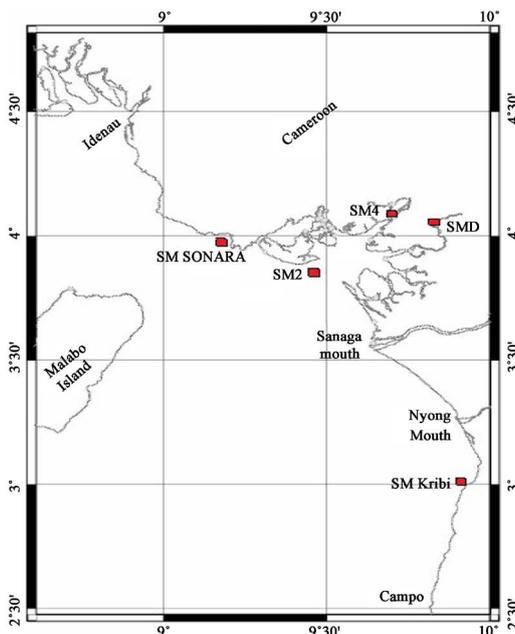
Figure 1. Map of the Cameroonian coast. The red points in the figure correspond to the location of the stations listed in **Table 1**.

different observation networks. Some locations are better surveyed than others. The Wouri estuary (SM2 and SM4 in **Figure 1**), for example has many tide gauges. In the north-west of the Cameroon coast (Limbe, SM SONARA), in the south (Kribi-Campo, SM KRIBI) and in Japoma water station in Dibamba (SMD), few measurements have been taken between 2007 and 2010. In all cases, the minimum duration of the recorded time series is six months. This period corresponds to the minimum duration required to perform an accurate harmonic analysis [7]. The paper is organized as follows: Section 2 presents the database. Section 3 addresses the harmonic analysis and prediction methods. Section 4 presents the resulting tidal constituents for the Cameroon coast and the related prediction. Section 5 focused on discussion and concludes paper.

2. Observations

2.1. Materials

The tide gauges installed in Cameroon use different technologies and measuring processes. A float type recorder using an analogue technology has been installed in Japoma water station in the Dibamba estuary (SMD in **Figure 1**).

The device consists of a float on a lever arm connected to a recorder (**Figure 2(a)**) and uses a still well to re-

(a)

(b)

(c)

(d)
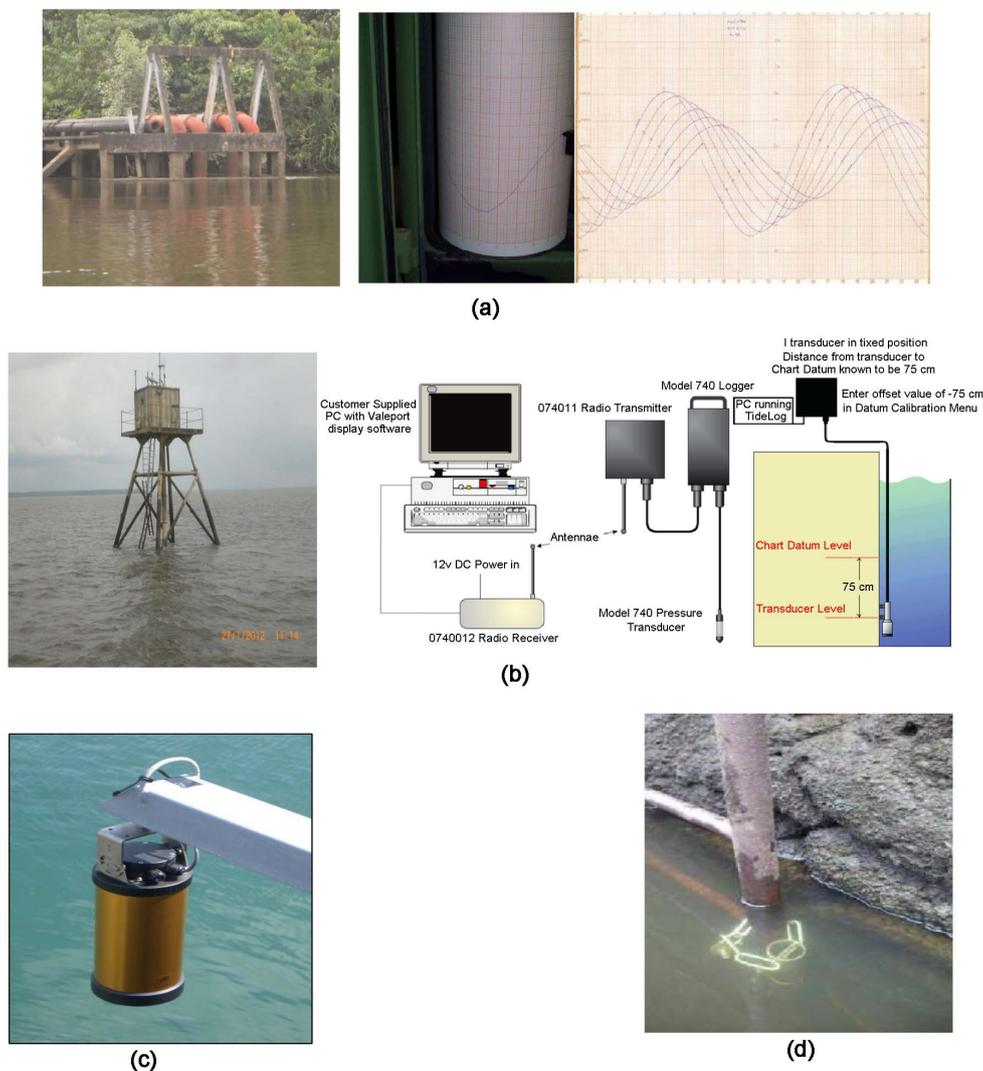
Figure 2. Tide gauge sensors installed in the Cameroonian coast: (a) Float type recorder (stations SM2, SM4, SMD) with analogue recorder; (b) Float type recorder (stations SM2, SM4) with digital recorder; (c) Radar sensor tide gauge (SM SONARA); (d) Pressure sensor installed on the bottom in the coastal water close to Kribi habour.

duce the effects of waves and wind. This type of sensor has also been installed at stations SM2 and SM4 (**Figure 1**) in the Wouri estuary.

The other tide gauge operate using numerical recorders and have two different measuring processes. The first process records the pressure at a fixed depth (for example on the bottom) and converts it to an equivalent sea level using the hydrostatic equation. The pressure sensor deployed in the Cameroon estuary is shown in **Figure 2(b)**. Raw data are sampled at 4 Hz and data logged as average over burst. Burst length is selectable between 1 to 60 seconds. This sensor is connected to a radio transmitter that communicates with a radio receiver connected to a computer. This model is installed at SM2 and SM4 stations (**Figure 1**). **Figure 2(d)** shows the one installed at Kribi during the period running from November 2009 to June 2010 (SM Kribi, see **Figure 1**). The last type is a very accurate radar sensor tide gauge (**Figure 2(c)**). This tidal gauge is part of the Global Sea Level Observing System network (GLOSS). It is installed at the SONARA refinery. This tide gauge is referenced in **Figure 1** by SM SONARA.

2.2. The Tide Dataset

The tide datasets used in this study covers the period 2007-2012. The years and the durations of the records are varying for each station. **Table 1** summarizes the positions of the tide gauges, the names of the stations, their characteristics and the measurement periods. In order to reduce the size of the dataset, the values are averaged over time. For Kribi and Limbe the data are sampled every fifteen minutes. For SM2 and SM4, the data are given every minute. Analogue tide gauge records at SM2, SM4 and SMD stations have been sampled manually with the time interval of 60 minutes. The data time series in the SMD station is short (eight months from January to August 2007) and includes large period of missing data, therefore the analysis derived from the measurements of this station is not very accurate.

3. Harmonic Analysis and Prediction Method

In order to provide the tide harmonic constants for the 5 stations along the Cameroon coast a tool developed at LEGOS laboratory has been used (for details on this tool, refer to ftp://ftp.legos.obs-mip.fr/pub/ecola/tools/ttb.pdf). The aim of harmonic analysis is to obtain significant and stable parameters describing the tidal regime at the place of observation [8]. This method is based on the assumption that the tidal variations can be represented by a finite number N of harmonic terms having the form:

$$H_n \cos(w_n t - G_n) \tag{1}$$

where H_n is the amplitude, G_n the phase lag defined using as a reference the tide phase at Greenwich, and w_n the angular speed. Harmonic constants are the solution of the following system expressed under its complex form, only applicable in case of the Darwin convention, described in Schureman (1940: pp. 74-79).

$$\left[v_n e^{j(w_n t + \Phi_n)} \right] [X_n] = [h_t] = \left[v_n e^{j(w_n t + V_0 - G_n)} \right] [X_n] \tag{2}$$

where v_n is a complex number giving the nodal correction in amplitude and phase, $[X_n]$ the harmonic coefficient vector linked to the gauge point, $[h_t]$ the time series vector, w_n the astronomic pulsation of the wave, t the time, V_0 the equilibrium argument at the time zero.

$$v_n = f_n e^{j u_n} \tag{3}$$

where f_n is the nodal factor and u_n the nodal angle. The nodal factor and the nodal angle are respectively equal to 1 and 0 for solar constituents. The Darwin spectrum needs at least an analysis over a 1 year period to be complete.

Table 1. Location and characteristics of the tide stations.

Station name	Instrument	Longitude	Latitude	Length series (days)	Sampling rate (min)	Period covered (year/month/days)
SM Kribi	Bottom sensor pressure	9.880E	2.928N	221	15	2009/11/01-2010/06/30
SM2	floatable tide gauge/model 740 water height	9.458E	3.794	575	1, 2, 5, 15, 60	2010/12/30-2012/09/15
SM4	floatable tide gauge/model 740 water height	9.667E	4.050N	607	1, 2, 5, 15, 60	2010/11/01-2012/09/17
SMD	floatable tide gauge	9.822E	4.041N	214	60	2007/01/21-2007/08/23
SM SONARA	Radar sensor	9.133E	4.004N	271	1, 2, 5, 15, 60	2008/06/01-2010/04/23

Taking M the matrix of harmonic vectors as:

$$M = \left[v_n \mathrm{e}^{j\left(w_n t + V_0 - G_n\right)} \right]$$

the solution is given by doing a standard least square fit by multiplying both sides with the transposed matrix of harmonic vectors M^*:

$$M^* M \left[X_n \right] = M^* \left[h_t \right] \tag{4}$$

When time series are shorter than 1 year, we used the admittance method developed by Cartwright *et al.*, 1980, which stipulates that the oceans and seas have a fairly smooth response. This means that the ratio of the amplitude over the astronomic potential of astronomic waves can be interpolated from their neighbours. This is useful when the length the data does not allow separating two constituents, which makes the matrix $M^* M$ singular or not invertible. An example is given by S2 and R2, which need 365.26 days to be separated when tide is regulary sampled. In this case, the R2 constituent from the nearest constituents N2 and M2 is expressed as:

$$\frac{\eta_{\mathrm{R2}}}{\Pi_{\mathrm{R2}}} = \frac{\dfrac{\eta_{\mathrm{N2}}}{\Pi_{\mathrm{N2}}}\left(\omega_{\mathrm{N2}} - \omega_{\mathrm{R2}}\right) + \dfrac{\eta_{\mathrm{M2}}}{\Pi_{\mathrm{M2}}}\left(\omega_{\mathrm{M2}} - \omega_{\mathrm{R2}}\right)}{\omega_{\mathrm{N2}} - \omega_{\mathrm{M2}}} \tag{5}$$

where Π the astronomic potential and η the tidal elevation at a certain location. A spline interpolation can also be used when there are 3 known components.

If the length of the data does not allow some components to be separated, $M^* M$ matrix is modified with the admittance method in order to be invertible. This method only applies to astronomic waves and cannot be used if they are contaminated by strong non-linear constituents. Therefore S2 cannot be used as input for the admittance method because it has a strong radiative component. Only M2, K2, N2, K1, O1, Q1, Mf, Mm and Mtm can be used as input waves for this method. The solution of harmonic analysis is finally given by:

$$\left[X_n \right] = \left(M^* M \right)^{-1} M^* \left[h_t \right] \tag{6}$$

According to [7]-[9], the prediction of the sea level at time t with N waves can be calculated as follows:

$$h(t) = H_0 + \sum_{n=1}^{N} X_n v_n e^{j\left(w_n t + V_0 - G_n\right)} + \varepsilon(t) \tag{7}$$

where H_0 is the mean level brought to zero of the local chard near to the gauged point and $\varepsilon(t)$ the random function used to represent storm surges. The harmonic analysis and the prediction require knowing in advance the astronomical potential amplitude and the angular speed and phase for each wave taken into account in the calculation. These parameters for the major tidal constituents given in [7]-[11] are recalled in **Table 2**.

The amplitude of the diurnal and semi-diurnal tide is modulation by slow variations associated with longer period motions of the Earth, Moon, and Sun [8]-[12]. These inter-annual tide modulation effects have been observed with two extensively documented signals (the 18.61-year lunar nodal cycle and the 8.85-year cycle of lunar perigee, see [13]-[16].

4. Results

4.1. Tide Constituents

The International Hydrographic Organisation (IHO) and Service Hydrographique et Océanographique de la Marine (SHOM) recommend the use of 500 waves to guarantee the quality of tidal predictions (see, e.g., http://www.iho.int/mtg_docs/com_wg/IHOTC/IHOTC_Misc/TWLWG_Constituent_list.pdf). However, the duration of the time series analysed here limits the number of tidal constituents that can be retrieved. Therefore the harmonic analysis method use in this study computes only 75 waves for the oceanic stations and 123 waves for the estuarine stations. This limits the spectrum to the eighth-diurnal period, which is sufficient in our framework because the amplitudes of waves having a shorter period are lower than 1 mm.

The amplitude and phase for each wave is computed for all stations and the results of the analysis for each station are presented in **Figure 3**. **Table 3** gives the tide constituents for waves having amplitude greater that 5 mm for each station. The tide constituents having the largest amplitudes are, as expected, the semi-diurnal, diurnal, fourth-diurnal and long term constituents. The results show that the tidal constituents in the Cameroon

Table 2. Principle astronomical harmonic components according to [7]-[11].

Origin	Symbol	Amplitude (cm)	Speed per mean (solar hour)	Period in solar (hours)
Long-period components				
Solar semi-annual	Ssa	1.9416	0.08213	2191.43
Lunar monthly	Mm	2.2056	0.54437	661.3
Lunar fortnightly	Mf	4.1765	1.09803	327.86
Diurnal components				
Larger lunar elliptic	Q1	1.9469	13.39867	26.87
Principle lunar diurnal	O1	10.0573	13.94303	25.82
Smaller lunar elliptic	M1	0.9788	14.49669	24.83
Principle solar diurnal	P1	4.6806	14.95893	24.07
Luni-solar diurnal	K1	14.1484	15.04107	23.93
Small lunar elliptic	J1	0.7921	15.58544	23.1
Semi-diurnal components				
Larger lunar elliptic	N2	4.6313	28.43973	12.66
Principle lunar	M2	24.2297	28.98411	12.42
Smaller lunar elliptic	L2	0.6694	29.52848	12.19
Larger solar elliptic	T2	0.6614	29.95893	12.02
Principle solar	S2	11.2734	30	12
Luni-solar semi-diurnal	K2	3.0697	30.08214	11.97
Lunarelliptic second order	2N2	0.6074925	27.89535	12.91
Lager lunar evectional	$\delta 2$	0.8747892	28.51258	12.63
Smaller lunar evectional	$\lambda 2$	0.1700979	29.45563	12.22
Variational	$\mu 2$	0.7532907	27.96821	12.87

Table 3. Tide constituents (amplitude and phase lag) for each station. Only waves with amplitude higher than 5 mm are shown. The phase lag is ranged between −180 and 180 deg.

		SM2		SM4		SMD		SM SONARA		SM Kribi	
	Freq (day^{-1})	Amplitude (m)	Phase (deg)	Amplitude (m)	Phase (deg)	Amplitude (m)	Phase (deg)	Amplitude (m)	Phase (deg)	Amplitude (m)	Phase (deg)
Waves					Long term period						
Sa	0.002737909			0.07578	−158.072754	0.190264	−80.539368	0.028401	20.058134		
Ssa	0.005475819	0.007687	42.954536	0.036737	12.337375	0.100593	57.196182	0.005422	116.489891	0.007381	−10.904999
MSm	0.031434739			0.011398	16.57612	0.129396	93.802628		−6.363464		
Mm	0.036291647			0.020014	15.562668			0.008269	29.390673		
MSf	0.067726386	0.010754	−62.647736	0.040768	24.943287	0.147646	28.927158	0.007251	20.715187	0.023358	138.084961
Mf	0.073202204	0.00954	−9.091461	0.02891	18.920385	0.029971	26.138809	0.007705	−13.745422		
MStm	0.104636944	0.015042	49.958076	0.011787	71.205215	0.016135	−9.56662	0.006403	53.383381		

Continued

Mtm	0.109493851	0.011614	39.282925	0.019286	45.073624	0.008186	58.259869	0.010182			
MSqm	0.14092859	0.00738	153.384537			0.014211	14.0913				
Mqm	0.145785497					0.024076	164.265945			0.012796	−160.470551
Diurnal constituents											
3OK1	0.783131297					0.020581	−106.268555				
2Q1	0.856952412					0.02133	−20.7229				
Sig1	0.86180932			0.006192	67.382446						
Q1	0.893244059			0.007513	140.326996	0.010157	−114.341736				
O1	0.929535705	0.026791	−23.277893	0.013543	−14.249207	0.009209	122.406006	0.027676	−29.403778	0.025983	−16.941772
MP1	0.935011524	0.002184	77.313423	0.00962	101.233139	0.031495	109.21917				
M1	0.966446262	0.008882	−15.389679	0.005606	25.525976	0.010364	−149.176041	0.006114	−51.141602	0.031945	−5.959045
Ki1	0.97130317					0.038151	−114.978256				
Pi1	0.994524312	0.022353	91.907127			0.028095	10.445965	0.011219	−14.583191	0.107726	−10.773438
P1	0.997262091			0.033058	−0.016357					0.038879	8.19433
S1	1			0.030791	110.527527						
K1	1.00273791	0.139004	4.684022	0.142374	17.69157	0.123573	52.335869	0.133466	−9.395264	0.124646	11.642342
Psi1	1.005475688			0.005892	92.079773						
Phi1	1.008213728	0.009153	80.388351			0.009443	29.250063				
Tta1	1.034172649					0.005814	−170.763123			0.008149	69.278305
J1	1.039029556	0.007404	23.285072	0.007999	61.356533	0.029671	132.472214	0.008272	11.299418		
SO1	1.070464295	0.006318	121.613472	0.011558	163.296112	0.016815	128.273834				
OO1	1.075940114	0.008613	61.583069			0.014988	106.887566	0.005243	54.445942	0.005073	−5.425293
KQ1	1.11223176									0.006591	144.726639
Semi diurnal constituents											
2MN2S2	1.760529196			0.005241	34.275955	0.079376	142.717484				
2NS2	1.791963936	0.012254	−164.195709			0.074297	130.67067	0.006182	27.464792		
ST1	1.797439756			0.008339	23.613209	0.06564	41.069794	0.007503	−5.853851		
OQ2	1.822779764	0.011944	65.236687	0.00927	98.224457	0.08898	−2.091461				
E2	1.828255583	0.010894	157.16861	0.019646	−111.563049	0.070775	−61.1362	0.005951	−26.848419	0.007223	79.189873
ST2	1.8337314	0.006497	−14.206512			0.12747	41.875446	0.005688	−127.485992		
ST3	1.853595591	0.012262	170.543411			0.1531	−107.041321	0.008109	−169.125839		
2N2	1.859690323	0.023646	126.31675			0.143334	40.31078	0.023456	86.435272	0.034589	134.164276
Mu2	1.864547229	0.024742	168.926514	0.065593	−136.861237	0.079857	−67.310791	0.026279	77.564034		
SNK2	1.890506149	0.021996	−70.888885			0.122139	39.674805	0.00578	79.357903		

Continued

N2	1.895981966	0.141372	133.567642	0.14479	147.574677	0.092689	−127.926086	0.132382	92.869659	0.121019	132.189606
Nu2	1.900838874	0.022171	169.496979	0.022628	111.870804	0.179889	−14.932648	0.027052	80.995308		
MSK2	1.926797796	0.047632	−159.039291	0.021932	−87.095764	0.046564	17.131142	0.007105	−45.030273		
M(SK)2				0.00999	−119.429352						
M2	1.932273613	0.711585	135.464478	0.815744	143.833298	0.65439	171.829712	0.593349	98.523415	0.542371	132.596161
M(KS)2	1.929535706			0.017438	85.859215						
MKS2	1.937749431	0.066651	−99.48291	0.014588	−35.520172	0.029719	−145.954041	0.013336	−52.061646		
La2	1.963708353	0.024569	101.929932	0.023706	137.666519	0.108169	−153.490616	0.010172	44.90461	0.004444	−173.808075
L2	1.968565261	0.039177	108.352959	0.062383	112.399132	0.064268	−30.623688	0.028233	93.301338		
T2	1.997262221	0.143218	66.034271	0.013105	179.454636	0.105576	−36.112213	0.079855	−127.520233	0.160296	176.641876
S2	2	0.505101	133.660629	0.253551	−171.965469	0.326837	−131.394409	0.470359	93.117485		
R2	2.002737779	0.180266	−18.038513			0.129407	9.780114	0.08383	109.193031		
K2	2.005475819	0.141372	133.567642	0.063171	177.545532	0.092689	−127.926086	0.132382	92.869659		
MSN2	2.036291645	0.017875	−59.420441	0.016815	−26.985901	0.08425	102.073799	0.015657	−48.752625		
KJ2	2.041767465	0.007177	110.102333			0.058359	−127.201416	0.012643	−120.723862	0.007626	94.449493
2SM2	2.067726384	0.01314	−1.4776	0.02372	4.497765	0.076771	69.776665	0.006553	−177.725998		
SKM2	2.073202203	0.019875	−33.248749	0.008382	14.604213	0.07141	−147.846771	0.007689	−170.932388		
2SN2	2.067726384					0.03817	149.046722				
2SMu2	2.135452773			0.006421	−179.707489	0.018901	−119.725739				
Third diurnal constituents											
MQ3	2.825517669	0.005341	109.894806	0.009677	82.473389	0.011415	136.620148				
2MK3	2.861809315	0.006797	106.774979	0.022386	84.032639	0.011734	129.458206				
M3	2.898410425			0.011023	−78.062988	0.013747	−109.625153				
SO3	2.929535702					0.008611	−178.511353				
MS3	2.932273614					0.011703	153.691772				
MK3	2.935011522			0.017891	1.720056						
SP3	2.997262094			0.004612	48.086643						
S3	3.000000003			0.001197	165.801666	0.0086	28.324894				
SK3	3.002737905			0.015935	83.434814	0.023646	−53.026245				
K3	3.008213726			0.002931	−85.822144	0.011614	−119.901962	0.019405	−77.265686		
Fourth diurnal constituents											
2MNS4	3.7605292			0.013675	−137.145401						
N4	3.79196394			0.005754	−87.806183	0.027267	6.949782				

Continued

Name	Freq	A1	P1	A2	P2	A3	P3	A4	P4	A5	P5
3MS4	3.796820848			0.023442	−135.321899	0.025397	15.914427			0.015005	−15.391602
MN4	3.828255588			0.025501	124.327751	0.027628	−58.121613				
MNu4	3.833112492	0.005113	56.394783	0.009812	86.393723	0.047516	30.198578				
M4	3.864547233			0.100709	136.856659	0.057839	−157.510391	0.035994	−28.834259	0.025912	30.459768
SN4	3.895981972			0.012422	−118.243271	0.038451	30.872028				
ML4	3.900838881	0.006141	85.841408	0.017518	99.765915	0.01917	−107.388184				
MS4	3.932273618			0.063054	−166.288055	0.043091	−84.799713	0.016706	42.691841	0.010486	112.544716
MK4	3.937749427	0.007193	157.130035	0.018265	−167.255432	0.017143	−155.441391				
2MSN4	3.968565264			0.010936	−23.551697	0.017349	93.9244				
S4	4			0.011209	−74.89267						
SK4	4.005475822					0.016331	−85.286957				
Sixth diurnal constituents											
3MNK6	5.687327004					0.006623	−79.681				
3MNS6	5.692802801					0.009426	−61.220795				
4MS6	5.729094441					0.009744	80.617027				
2MN6	5.760529202			0.006025	138.051956	0.00868	−26.235291				
2MNu6	5.76538611					0.015517	82.185829				
3MSK6	5.79134502					0.010763	−141.661774				
M6	5.79682085	0.010779	−29.251007			0.0128	−79.479095	0.012588	−80.157043		
3MKS6	5.802296674					0.016884	104.463013				
MSN6	5.828255587			0.005209	−164.014648						
2ML6	5.833112482					0.014841	−93.343933				
2MS6	5.864547244	0.008201	17.890024	0.016267	−168.859131	0.017168	−41.666199	0.01034	−18.480988		
2MK6	5.870023061			0.005239	−150.652023	0.00604	168.72467				
MSL6	5.900838881					0.0128	−118.931458				
3MSN6	5.900838881					0.009282	−144.562698				
2SM6	5.932273617			0.005801	−112.146835	0.008563	−17.60141				
MSK6	5.937749419					0.005076	21.206036				
Eight diurnal constituents											
M8	7.729094436			0.006018	94.106453	0.006936	−123.32019				
3ML8	7.765386128					0.007524	−12.517822				
3MS8	7.796820837			0.007055	139.444321	0.005847	−18.517334				
2M2S8	7.802296668					0.006156	149.249374				
2MSK8	7.864547205					0.00846	−58.470337				
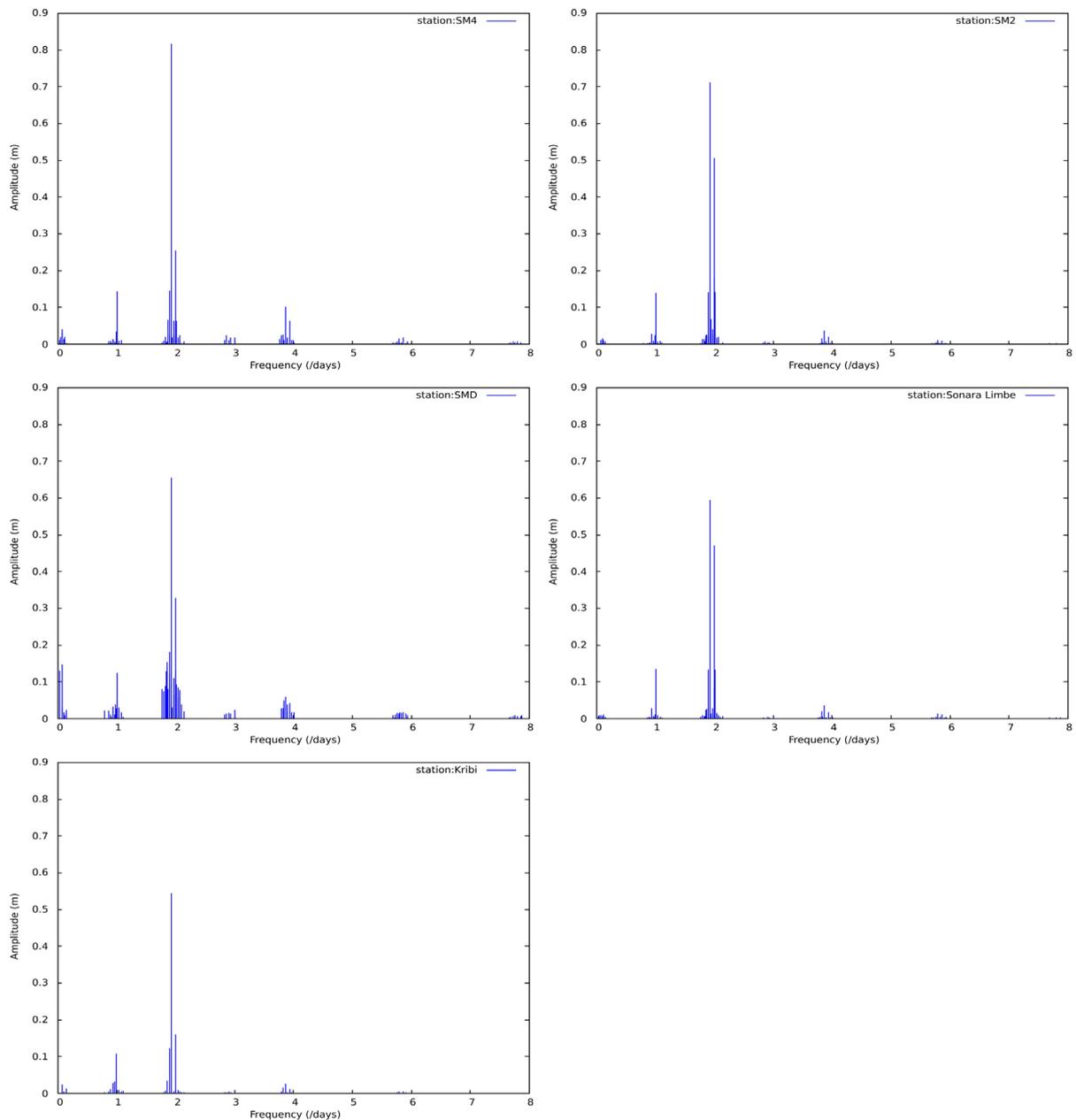
Figure 3. Amplitude spectrum of tide for the five stations whose location is given in **Figure 1**.

coast are moderated with average amplitude of the M2 tide equal to 0.5 m over the continental slope. This confirms the results of the tide atlas build by [6]. The tide is amplified in the shallow water of estuaries and its peak is observed in the Wouri (SM4) and Dibamba (SMD) estuaries because of the strong convergence of these bays. The minimum is observed at the Kribi station located in the South coast. Over all the stations, the M2 tide amplitude ranges between 0.5 and 0.85 m.

The S2 constituent varies similarly as the M2 constituent. Its amplitude ranges between 0.18 and 0.52 m. The lowest S2 amplitude occurs also at Kribi station and the maximum occurs in Cameroon estuary. At the Japoma water station, in addition to the classic M2 and S2 components, the spectrum shows a large number of semi-diurnal waves (ST2, 2N2 SNK2, Nu2, R2, LA2, T2 and MSN2) with amplitude higher than 0.1 m (**Figure 3**). This explains the larger tide amplitude observed in this location compared to other stations despite relatively smaller M2 and S2 amplitudes. The major diurnal wave in the Cameroon coast is the K1 tide with an amplitude of the

order of 0.14 m and its amplitude is homogeneous along the coast.

The fourth-diurnal waves are amplified in the estuary. In this group, the M4 tide is the major component. **Figure 3** shows that the amplitudes of the fourth-diurnal waves in the estuary stations (SM4 and SMD) are higher than the ones of the stations located in the continental slope (SM2, SM-Kribi and SM-SONARA). **Figure 3** also shows that long-term components (Sa, Ssa, Msm and Msf) at the SMD station have a higher amplitude than other stations. As shown in **Figure 1**, this station is located upstream in the Dibamba river, therefore this result can be explained by the strong fluctuations of the river run-off and non-linear interactions between M2 and S2 tides occurring in shallow waters. For example, the amplitude of the Msf tide that is due to these non-linear effects is equal to 0.14 m and therefore not negligible.

Comparatively, in coastal zones out of estuaries the amplitudes of the lunar-solar fortnightly Msf (corresponding to a 14.765 day period) and the lunar fortnightly Mf (corresponding to a 13.661 day period) is of the order of 1 cm. However, as explained above, the harmonic analysis of the data collected at the SMD station needs to be confirmed with longer records.

4.2. The Effect of the Hourly Averaging

Usually the harmonic analysis method is applied to hourly data. However, in estuaries, the high frequency constituents of tide (above the fourth-dirunal constituent) have an important amplitude (see the previous section).

Therefore the use of hourly average data may introduce a non negligible error in the analysis compared to using the raw data sampled at a 1mn time interval. This problem may affect the SM2, SM4 and SMD station in the Cameroon estuary.

In order to investigate the impact of the hourly average, the harmonic analysis is performed on two datasets collected at the SM2 and SM4 stations equipped with a numerical recorder. The SM2 dataset corresponds to the raw data sampled at a 1mn time interval and the second corresponds to the hourly average of these raw data. **Figure 4** and **Figure 5** show the differences of the tide constituents amplitude and phase between the two sample periods for the two stations. The amplitude difference is of the order of 1 cm for major waves. However, at the SM2 station, the R2 and T2 tide amplitudes present significant differences, respectively equal to 0.16 and 0.14 m, which were not expected. The scatter plot presented in **Figure 4(a)** also shows that there is a non negligible phase shift between the two datasets at SM2 station. These differences indicate that the quality of the SM2 data are questionable, which will be discussed in the next section. As to the SM4 data, the amplitude difference is very small over all the frequencies and the scatter plot presented in **Figure 5(a)** shows that the phase shift is not significant, except for a few waves.

Despite the fact that the SM4 station is located upstream in the Wouri estuary and that, as a consequence, its spectrum exhibit important high frequency harmonics, the results obtained with the hourly SM4 data are comparable to those obtained with a 1mn sampling interval. This suggests that we can provide an accurate harmonic analysis using hourly data even in the estuaries, which allows collecting longer time series due to the limited memory required to store this type of data.

4.3. Prediction of Tides

The quality of the tide constituents obtained by harmonic analysis is evaluated by reconstructing the tidal signal and comparing it to the data. The prediction of tides is realized with a tool developed at LEGOS (for details on this tool, refer to ftp://ftp.legos.obs-mip.fr/pub/ecola/tools/ttb.pdf). The results are satisfactory for the SM-SONARA, SM-Kribi and SM4 stations (**Figure 6**). The observed tide and the predicted tide are perfectly in phase and the difference between the two signals is a residual noise. The amplitude of these differences can be up to 0.2 m at low and high tides.

However, **Figure 6(a)** shows that the prediction is not accurate for the SM2 station operated by the Douala harbour. The amplitude of the difference between the predicted tide and the data reaches 0.5 m at low and high tides. The residual clearly includes an important part of the dominant components, which implies that the harmonic analysis does not correctly extract the tide for this station. This problem had already been noticed in the previous section where the amplitude of the R2 and T2 constituents for this station was found to be ten times greater than the ones of the others stations. These values are therefore unrealistic and can be the cause of the high prediction error.

One of the typical problems in the observation of tides is due to a shift of the reference time. **Figure 7** indeed
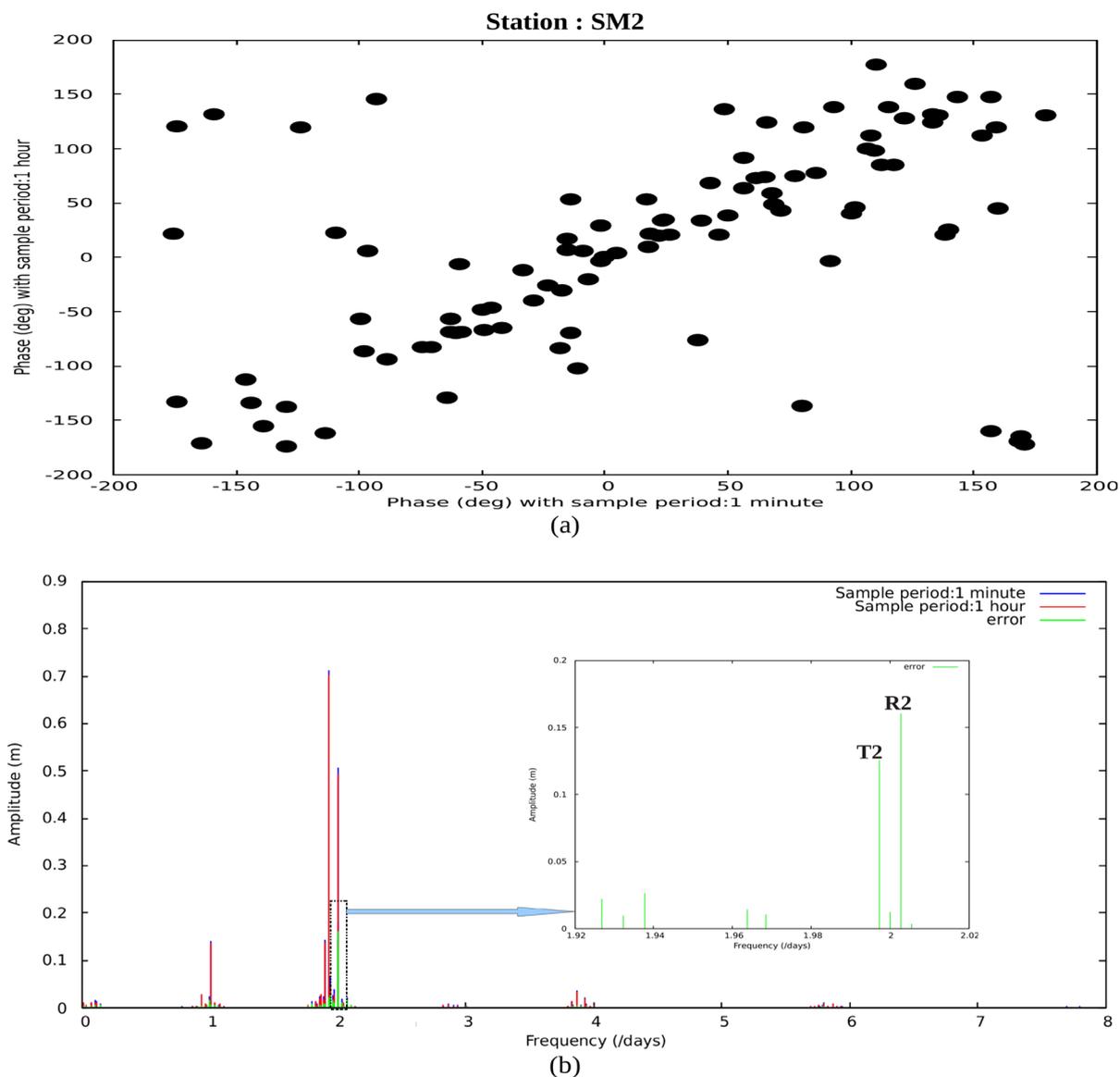
Figure 4. Comparison between the harmonic analysis results computed with data sampled at 1 minute and data averaged at a 1h time scale at the station SM2. The scatter plot (a) gives the phase for the 1 h averaged data as a function of the phase for raw data for each constituent. The spectrum (b) shows the constituents amplitudes for 1h averaged data (red), raw data (blue) and their differences (green).

shows several time shifts in the dataset measured at the SM2 station. We need to fix in order to recompute the tide constituents. To investigate this hypothesis, the time derivative of the sea surface height was computed in order to locate sudden jumps in the data, which is possible because the tide involves only slow changes of height. This analysis is presented in **Figure 7** which shows that the peaks in the time derivative correspond very well to the errors in data. Five major anomalies were detected and were found to be an increase or a decrease of one hour in the reference time. These anomalies always occur in the first day or last day of the month, which suggests that they could be caused by the operator during maintenance activities. After correction of these spurious jumps, the T2 and R2 tides constituents fell down to 1.5 and 0.2 cm respectively. The M2 amplitude also increases from 0.71 to 0.75 m and its phase from 135.46˚ to 149.1˚. **Table 4** shows the corrected major tides constituents for the SM2 station. As expected, the amplitude of the corrected residual is consequently reduced (see **Figure 8**).

(a)

(b)
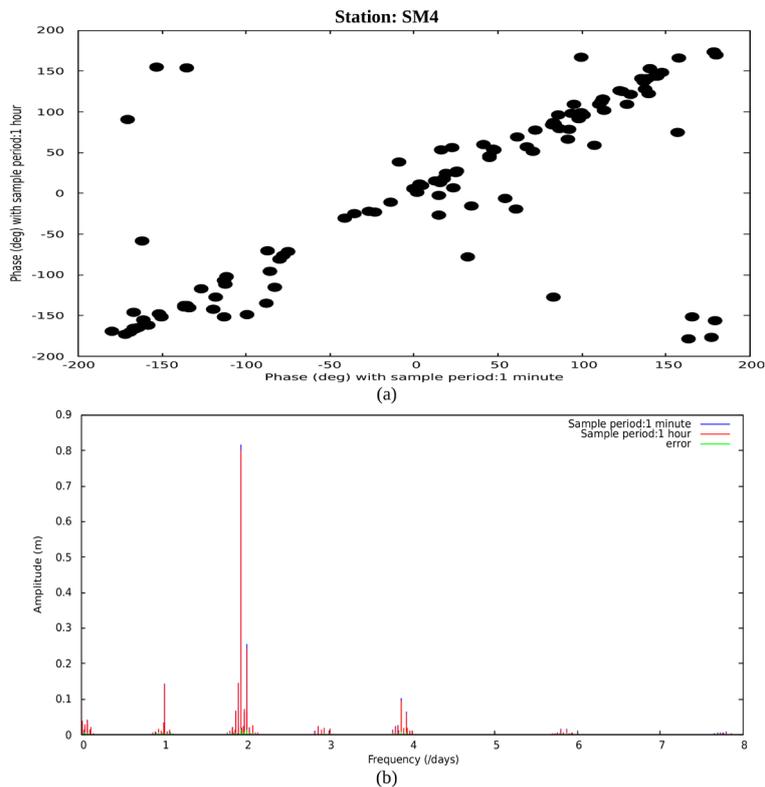
Figure 5. Comparison between the harmonic analysis results computed with data sampled at 1 minute and data averaged at a 1 h time scale at the station SM4. The scatter plot (a) gives the phase for the 1 h averaged data as a function of the phase for raw data for each constituent; The spectrum (b) shows the constituents amplitudes for 1 h averaged data (red), raw data (blue) and their differences (green).

(a)

(b)

(c)

(d)
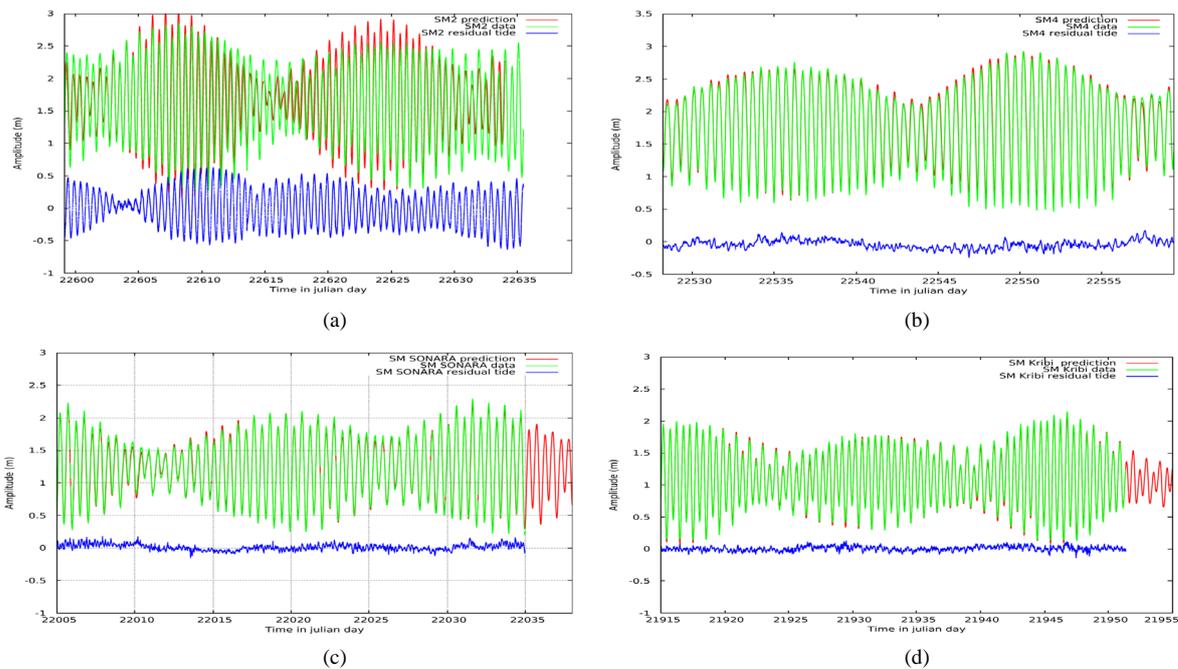
Figure 6. Observed tide (green curve), predicted tide (red curve) and residual (blue curve) as a function of time in julian day at: (a) SM2 station; (b) SM4 station; (c) SM SONARA station; (d) SM Kribi station.
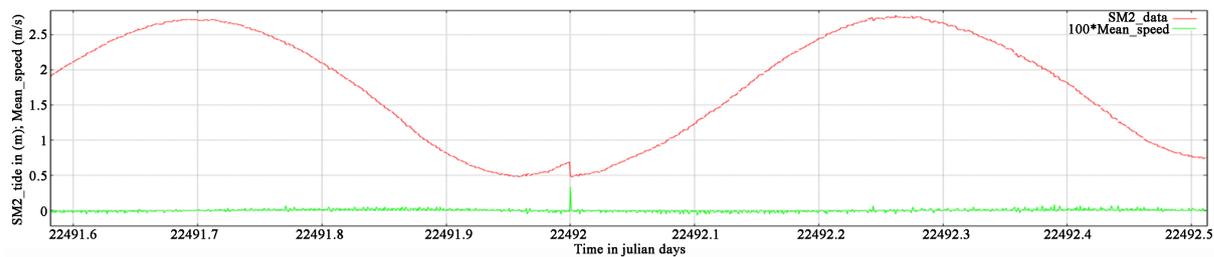
(a)
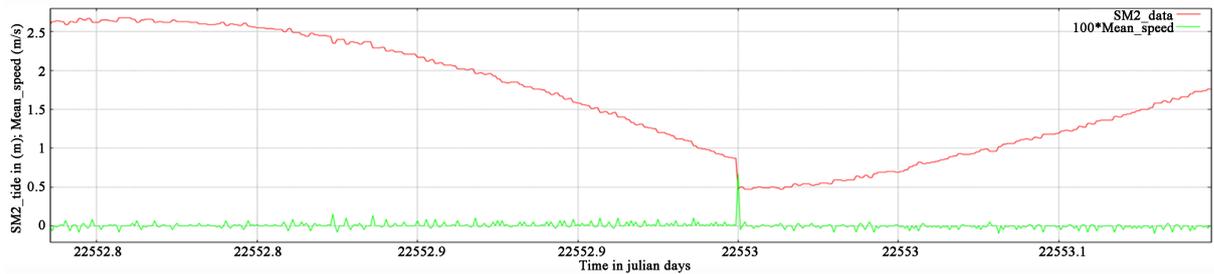
(b)
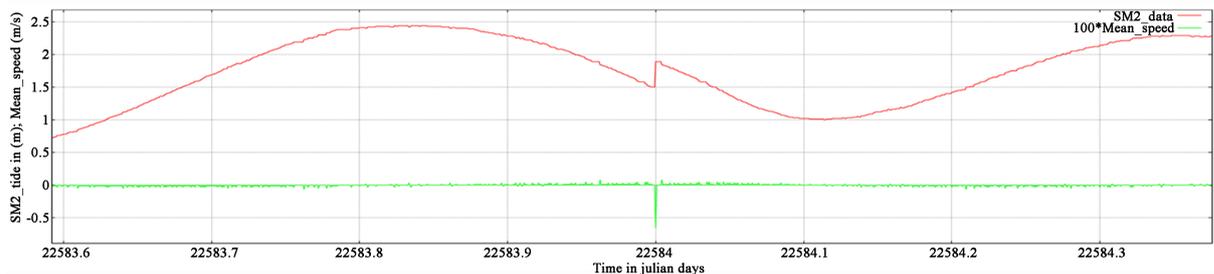
(c)
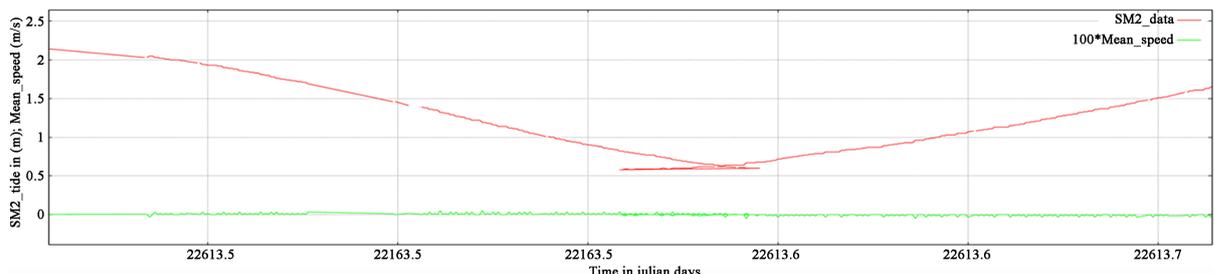
(d)
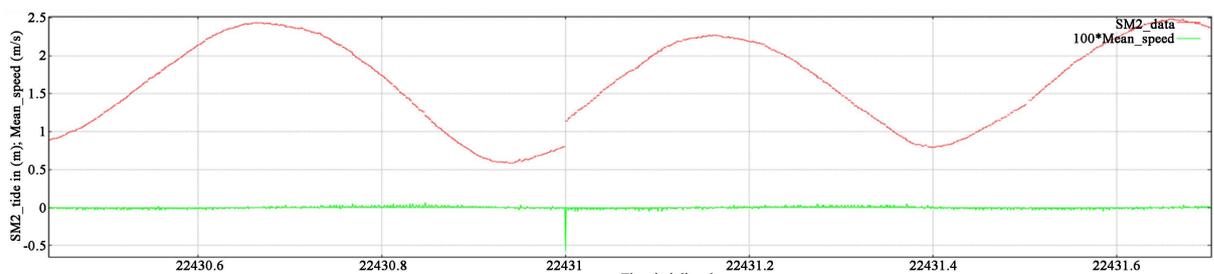
(e)

Figure 7. Tidal height measured at the SM2 station (in meter, red curve) and time derivative (in cm·s^{-1}, green curve) for various days (a); (b); (c); (d) and (e).

Table 4. Tide constituents (amplitude and phase lag) for SM2 station with corrected data. Only waves with amplitude higher than 5 mm are shown. The phase lag is ranged between −180 and 180 deg.

Waves	SM2				SM2		
	Freq (day^{-1})	Amplitude (m)	Phase (deg)		Freq (day^{-1})	Amplitude (m)	Phase (deg)
	Long term period				**Semi diurnal constituents**		
Ssa	0.005475819	0.007687	42.954536	N2	1.895981966	0.147252	146.529419
MSm	0.031434739	0.009431	22.069765	Nu2	1.900838874	0.024988	145.514008
MSf	0.067726386	0.010754	−62.647736	MSK2	1.926797796	0.047632	−159.039291
Mf	0.073202204	0.011458	−10.49649	M2	1.932273613	0.749268	149.19809
MStm	0.104636944	0.015042	49.958076	MKS2	1.937749431	0.066651	−99.48291
Mtm	0.109493851	0.010452	46.35207	La2	1.963708353	0.024569	101.929932
MSqm	0.14092859	0.00577	154.245758	L2	1.968565261	0.036254	141.659775
	Diurnal constituents			T2	1.997262221	0.015466	176.56662
Q1	0.893244059	0.005339	138.39241	S2	2	0.252474	−173.564209
O1	0.929535705	0.026136	−16.858978	R2	2.002737779	0.002139	−179.330322
MP1	0.935011524	0.002184	77.313423	K2	2.005475819	0.069793	−177.184799
M1	0.966446262	0.008882	−15.389679	MSN2	2.036291645	0.017875	−59.420441
Pi1	0.994524312	0.022353	91.907127	KJ2	2.041767465	0.007177	110.102333
P1	0.997262091	0.042862	18.367414	2SM2	2.067726384	0.01314	−1.4776
K1	1.00273791	0.137472	16.627121	SKM2	2.073202203	0.019875	−33.248749
Phi1	1.008213728	0.009153	80.388351		**Third diurnal constituents**		
J1	1.039029556	0.007404	23.285072	MQ3	2.825517669	0.005341	109.894806
SO1	1.070464295	0.006318	121.613472	2MK3	2.861809315	0.006797	106.774979
OO1	1.075940114	0.008613	61.583069		**Fourth diurnal constituents**		
	Semi diurnal constituents			MNu4	3.833112492	0.005113	56.394783
2NS2	1.791963936	0.012254	−164.195709	M4	3.864547233	0.042206	95.232109
ST1	1.797439756	0.003907	139.768997	ML4	3.900838881	0.006141	85.841408
OQ2	1.822779764	0.011944	65.236687	MS4	3.932273618	0.021467	150.431839
E2	1.828255583	0.010894	157.16861	MK4	3.937749427	0.007193	157.130035
ST2	1.8337314	0.006497	−14.206512		**Sixth diurnal constituents**		
ST3	1.853595591	0.012262	170.543411	M6	5.79682085	0.010779	−29.251007
2N2	1.859690323	0.02031	129.042831	2MS6	5.864547244	0.008201	17.890024
Mu2	1.864547229	0.020418	−174.405853	2MS6	5.864547244	0.008201	17.890024
SNK2	1.890506149	0.021996	−70.888885				
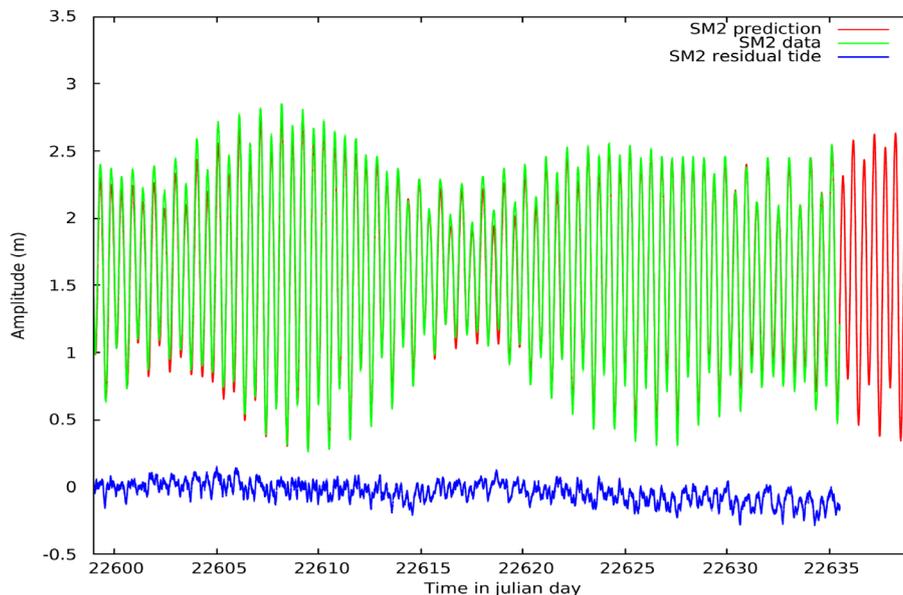
Figure 8. Observed tide (green curve), predicted tide (red curve) and residual (blue curve) as a function of time in julian day at the SM2 station after correction of the spurious jumps.

5. Discussion and Conclusion

Harmonic analysis allows extracting the tidal constituents and predicting the sea level height. However, this method does not extract perfectly all the amplitude of the tide constituents. As can be seen in **Figure 6** and **Figure 8**, the residuals still include both low and high frequencies. A Demerliac filter can be applied to remove the low frequency signal from the residuals [17]. The difference between the residuals and the filtered signal can be added to the prediction of the tide.

This correction can have great interest for sea surface height data assimilation and adjustment of numerical tidal model that require high quality tide predictions. The remaining high frequencies of the residuals are more difficult to analyse because one part is due to the atmospheric forcing and another to the tidal forcing.

The records used in this study are not long enough to allow the very long-term constituents to be retrieved with harmonic analysis. For example, the lunar nodal, nodal sub-harmonic, lunar perigean, and perigean sub-harmonic cycles (corresponding to 18.6, 9.3, 8.85, and 4.4-year signals respectively [18] [19]) cannot be obtained. Moreover, the diurnal and semi-diurnal tides are modulated over a large range of time scales including annual and inter-annual variations [20] and these cycles constituents requires dedicated techniques to be retrieved.

Although harmonic analysis combined with the admittance method shows accurate results with relatively short time series, these results are less reliable in the more non-linear and mixed semi-diurnal zone of the Cameroon estuary. Indeed, the harmonic components in shallow water are not only astronomical. For example, the S2 component is strongly astronomic, but also radiational and includes non-linear combinations like S1 + S1, S3 − S1 and K1 + P1. M2 also includes a non-astronomical combinations of K1 + O1, N2 a combination of M1 + O1 and K1 a combination of S2 − P1. Therefore the resulting prediction can be inaccurate when it is performed over interval for which there is no available data.

The scope of this study is also limited due to the fact that tide gauges are sparse in Cameroon coastal areas. It is therefore of primary importance to build a more dense network of sea level gauges. This project would have to be designed and implemented with consideration for at-risk areas to complement the existing system.

In conclusion, the harmonic analysis method has been used to extract the tide constituents for five stations along the Cameroon coast. After corrections, particularly on the SM2 dataset, the prediction of tide derived from the analysis gave very accurate results compared to the data. However, the SMD station was only equipped with an analogue recorder and therefore the results for this station are less satisfactory due to the short duration of the recorded data and the important number of missing data. The use of hourly data instead of data sampled at 1 mn was found to generate negligible errors in harmonic analysis, even in estuaries where high frequency waves have

a larger amplitude.

The maximum tide height in the Cameroon coast is observed in Cameroon estuary. In Limbe (SM SONARA) the tide amplitude is smaller but bigger than the one observed in the south coast (SM Kribi). The amplitudes of the fourth-diurnal waves in the estuary stations (SM4 and SMD) are higher than the ones of the stations located in the continental slope, which can be explained by non-linear interactions between M2 and S2 tides occurring in shallow waters. The strong fluctuations of rivers run-off also affects the long-term components of the tide, which can be observed at the SMD station located upstream in the Dibamba river.

Acknowledgements

References

[1]   Fonteh, M., Esteves, L.S. and Gehrels, W.R. (2009) Mapping and Valuation of Ecosystems and Economic Activities along the Coast of Cameroon: Implications of Future Sea Level Rise. EUCC—Die Küsten Union Deutschland e.V.: International Approaches of Coastal Research in Theory and Practice. *Coastline Reports*, **13**, 47-63.

[2]   Asangwe, C.K. (2006) The Douala Coastal Lagoon Complex, Cameroon: Environmental Issues, Administering Marine Spaces: International Issues. FIG publication No. 36.

[3]   Jean, F., Mbome, L., Bokwe, A. and Tangang, A. (1999) Profil côtier du Cameroun, Projet Grand Ecosystème Marin du Golfe de Guinée. Ministère de l'Environnement et des Forêts. Yaoundé, Cameroun, 106 p.

[4]   Olivry, J.C. (1974) Hydrologie du bief maritime de la Dibamba en periode d'étiage, note sur les étiages du mungo 9, ed. Mesres-Orstom, Paris.

[5]   Olivry, J.C. (1986) Fleuves et Rivières du Cameroun. Collection Monographie Hydrologique 9, ed. Mesres-Orstom, Paris.

[6]   Onguene, R., Duhaut, T., Lyard, F., Marsaleix, P., Allain, D, Pemha, E., Njeugna, E., Nguyen, C. and Du-Penhoat, Y. (2013) Hydrodynamic and Salinity Modeling of Estuaries in Central Africa. Application to the Cameroon Estuaries. *3rd JEAI-ALOC_GG International Workshop*, Cotonou, 3-8 2013.

[7]   Schureman, P. (1940) Manual of Harmonic Analysis and Prediction of Tides. United States Government Printing Office, 317 p. (reprinted with correction, 1976) United States Coast and Geodetic Survey Special Publication No. 98, Department Of Commerce, Washington DC.

[8]   Pugh, D. (1987) Tides, Surges and Mean Sea-Level. John Wiley, London.

[9]   Simon B. (2007) La marée océanique côtière. In: Institut Océanographique, Ed., Collection "*Synthèses*", Paris, 433 p.

[10] Defant, A. (1961) Physical oceanography. Pergamon Press, New York.

[11] Manasrah (2013) Tide Variation and Signals during 2000-2004 in the Northern Gulf of Aqaba, Red Sea. *Natural Science*, **5**, 1264-1271. http://dx.doi.org/10.4236/ns.2013.512154

[12] Wood, F. (2001) Tidal Dynamics: Theory and Analysis of Tidal Forces. *Journal of Coastal Research*, **1**, Coastal Education Research Foundation, West Palm Beach, Fla.

[13] Araujo, I.B. and Pugh, D.T. (2008) Sea Levels at Newlyn, 1915-2005: Analysis of Trends for Future Flooding Risks. *Journal of Coastal Research*, **24**, 203-212. http://dx.doi.org/10.2112/06-0785.1

[14] Boon, J.D. (2004) Secrets of the Tide: Tide and Tidal Current Analysis and Applications, Storm Surges and Sea Level Trends. Ellis Horwood, Chichester.

[15] Shaw, A.G.P. and Tsimplis, M.N. (2010) The 18.6 yr Nodal Modulation in the Tides of Southern European Coasts. *Continental Shelf Research*, **30**, 138-151. http://dx.doi.org/10.1016/j.csr.2009.10.006

[16] US Army Corps of Engineers (1989) Water Levels and Wave Heights for Coastal Engineering Design. US Army Corps of Engineers, Hyattsville.

[17] Demerliac, M.A. (1974) Calcul du niveau moyen journalier. Annales Hydrographiques du SHOM 5 éme série, 49-57.

[18] Pugh, D. (2004) Changing Sea Levels, Effects of Tides, Weather and Climate. Cambridge University Press, Cambridge, 280 p.

[19] Wood, F. (2001) Tidal Dynamics: Extreme Tidal Peaks and Coastal Flooding. *Journal of Coastal Research*, 2, Coastal

Education Research Foundation, West Palm Beach, Fla.

[20] Doodson, A.T. (1921) Harmonic Development of the Tide-Generating Potential. *Proceedings of the Royal Society of London A*, **100**, 305-329. http://dx.doi.org/10.1098/rspa.1921.0088